

Anisotropic flow of identified particles in Pb–Pb collisions at $\sqrt{s_{\text{NN}}} = 5.02$ TeV

Redmer Alexander Bertens^{1,*}

¹University of Tennessee (Knoxville, USA)

Abstract. Anisotropic flow is sensitive to the shear (η/s) and bulk (ζ/s) viscosity of the quark-gluon plasma created in heavy-ion collisions, as well as the initial state of such collisions and hadronization mechanisms. In these proceedings, elliptic (v_2) and higher harmonic (v_3, v_4) flow coefficients of π^\pm , K^\pm , $p(\bar{p})$ and the ϕ -meson, are presented for Pb–Pb collisions at the highest-ever center-of-mass energy of $\sqrt{s_{\text{NN}}} = 5.02$ TeV. Comparisons to hydrodynamic calculations (IP-Glasma, MUSIC, UrQMD) are shown to constrain the initial conditions and viscosity of the medium.

1 Introduction

Ultra-relativistic heavy-ion collisions are used to study the properties of the quark-gluon plasma (QGP), a state of deconfined quarks and gluons that is created at high energy densities and temperatures. Past measurements of azimuthal anisotropies in particle production relative to collision symmetry plane angles Ψ_n have shown that the QGP behaves as a nearly perfect fluid [1]. These anisotropies in particle production arise when initial spatial anisotropies, resulting from the approximately elliptic overlap region of the colliding nuclei in non-central collisions, combined with the initial inhomogeneities of the system density, are transformed, through multiple interactions between the produced particles, into an anisotropy in momentum space. The efficiency of this process depends on the system's transport coefficients such as shear (η/s) and bulk (ζ/s) viscosity.

Momentum anisotropy in particle production is quantified as harmonic coefficients v_n of a Fourier series of the azimuthal angle (φ) distribution relative to the system's symmetry plane angles Ψ_n [2]

$$\frac{dN}{d(\varphi - \Psi_n)} \propto 1 + \sum_{n=1}^{\infty} 2v_n \cos(n[\varphi - \Psi_n]). \quad (1)$$

Harmonic coefficients v_n – commonly called *flow coefficients* – are, in addition to being a probe for η/s and ζ/s , also sensitive to the initial state of the system, freeze-out conditions, hadronization mechanisms, and the lifetime of the system.

2 Data analysis

A sample of Pb–Pb collisions used for this work were recorded with the ALICE [3] detector at a center of mass energy per nucleon pair of $\sqrt{s_{\text{NN}}} = 5.02$ TeV. The data set comprises $\approx 6 \times 10^7$ collisions with

*e-mail: rbertens@cern.ch

a primary vertex reconstructed within ± 10 cm along the beam pipe. The Inner Tracking System (ITS) and Time Projection Chamber (TPC) are used to reconstruct charged particles at $|\eta| < 0.9$ and $|y| < 0.5$. The V0 scintillator detectors, located at $2.8 < \eta < 5.1$ (V0A) and $-3.7 < \eta < -1.7$ (V0C), are used for centrality determination, and reconstruction of the \mathbf{Q}_n^{V0} vectors (see Eq. 2). Particle identification is performed using ionization energy loss measured in the TPC, combined with the arrival time of particles in the Time of Flight (TOF) detector. The ϕ -meson is reconstructed in the $\phi \rightarrow K^+K^-$ channel, using the analysis method outlined in [4].

The scalar product method [5] is used to measure flow coefficients v_n , and is defined as

$$v_n\{\text{SP, V0C}\} = \langle\langle \mathbf{u}_n \cdot \mathbf{Q}_n^{\text{V0C}*} \rangle\rangle \left/ \sqrt{\frac{\langle \mathbf{Q}_n^{\text{V0C}} \cdot \mathbf{Q}_n^{\text{TPC}*} \rangle \langle \mathbf{Q}_n^{\text{V0C}} \cdot \mathbf{Q}_n^{\text{V0A}*} \rangle}{\langle \mathbf{Q}_n^{\text{TPC}} \cdot \mathbf{Q}_n^{\text{V0A}*} \rangle}} \right., \quad (2)$$

where $\mathbf{u}_n = \exp(in\varphi)$, in which φ represents azimuthal angle, is the unit vector of a particle of which v_n is measured. Reference flow vectors $\mathbf{Q}_n = \sum_j \exp(in\varphi_j)$ (the sum runs over all j tracks and * denotes the complex conjugate) are measured in the TPC and V0 detectors, where V0C is chosen as reference flow detector as it still has a high event plane resolution. The large rapidity gap between \mathbf{u}_n and $\mathbf{Q}_n^{\text{V0C}*}$ ensures that contributions of short-range correlations that are unrelated to the initial geometry – ‘non-flow’ – are suppressed.. Brackets $\langle \dots \rangle$ in Eq. 2 represent an all-event average; the double brackets in the numerator indicate that prior to the all-event average, an average over all $\mathbf{u}_n \cdot \mathbf{Q}_n^{\text{V0C}*}$ within the single event is taken.

3 Results

Figure 1 shows p_T -differential v_2 (top panel) of π^\pm , K^\pm , $p(\bar{p})$ and the ϕ -meson for 10-20% (left) and 40-50% (right) collision centralities. For $p_T < 4$ GeV/c, only \bar{p} are considered to exclude a contamination from detector material. A mass splitting of v_2 of different particle species is found for $p_T < 2$ GeV/c, which is indicative of strong radial flow [6]. For $3 < p_T < 8$ GeV/c the curves for different particles group according to their constituent quark number, supporting the concept of particle production via quark coalescence [7]. Flow of the ϕ -meson most directly illustrates mass splitting and quark number scaling since the ϕ is a meson with a mass close to proton mass. The ϕ -meson v_2 indeed follows proton v_2 at low p_T , but pion v_2 at intermediate p_T . The fact that $p(\bar{p})$ v_2 is larger than π^\pm v_2 for $3 \lesssim p_T \lesssim 10$ GeV/c, after which the v_2 converge, suggests that partonic energy loss is flavor independent at high p_T .

Inhomogeneities in the initial nucleon distribution produce higher harmonic flow coefficients ($n > 2$). These coefficients are thought to be more sensitive to transport coefficients than v_2 [8]. Non-zero v_3 is observed for π^\pm , K^\pm , $p(\bar{p})$ up to $p_T \approx 8$ GeV/c, as is shown in the middle panel of Fig. 1; v_4 is non-zero in the entire measured range ($p_T < 4$ GeV/c, lower panel). The aforementioned mass splitting is visible for v_3 and v_4 up to $p_T \approx 2.5$ GeV/c.

Model predictions from [9] are shown to test the validity of the hydrodynamic description of the QGP in Fig. 2. The curves are based on an IP-Glasma initial state and use a viscous hydrodynamic medium evolution ($\eta/s = 0.095$ with a temperature-dependent ζ/s), followed by a hadronic cascade procedure for hadronization. Mass splitting is violated (ϕ -meson $v_2 > p(\bar{p})$ v_2) in the model, likely resulting from an under-prediction of the hadronic cross section of the ϕ -meson. The model is in agreement with the data for $p_T < 1$ GeV/c in central collisions, but overestimates v_2 already at lower p_T for more peripheral collisions.

To test the hypothesis of particle production via quark coalescence, the axes of Fig. 1 are scaled by the number of constituent quarks n_q independently for each species [7] in Fig. 3. From $p_T/n_q > 1.5$ GeV/c particles group approximately according to their type (baryon, meson). Similar behavior is

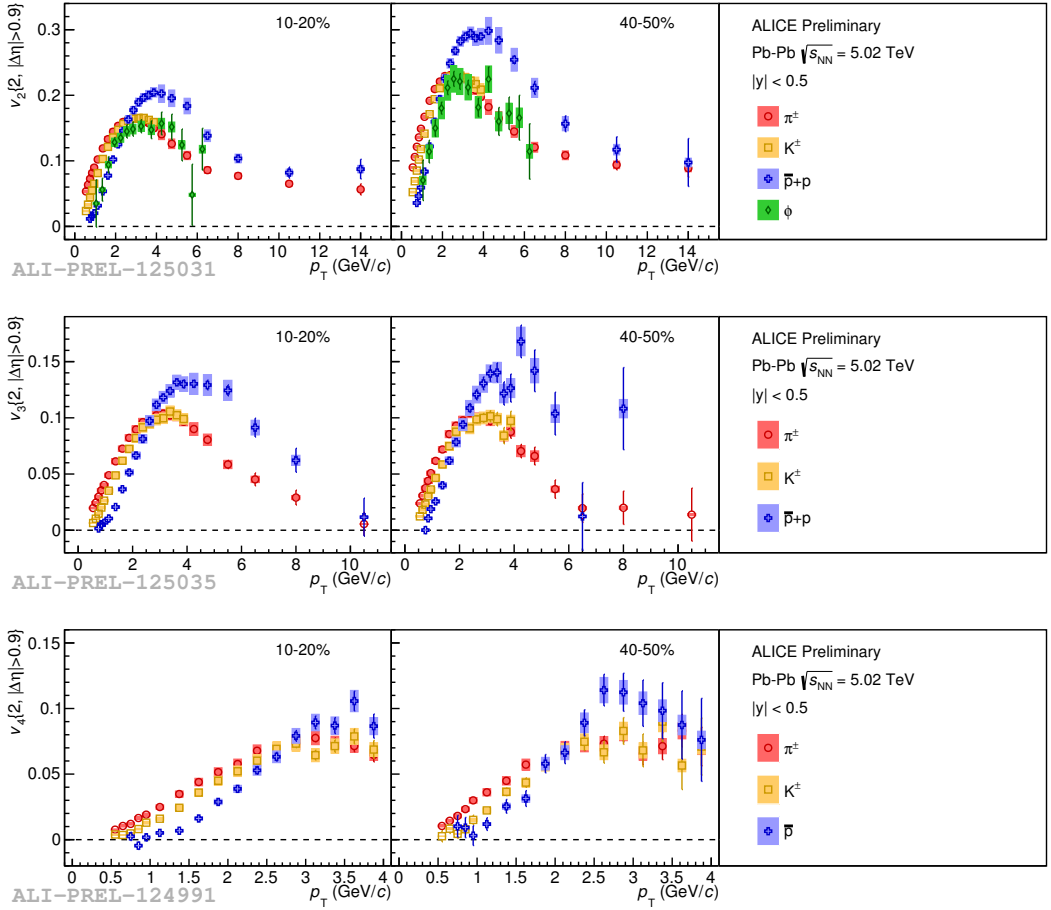


Figure 1. Flow coefficient v_2 (top), v_3 (middle) and v_4 (bottom) of π^\pm , K^\pm , $p(\bar{p})$ and the ϕ -meson for 10-20% (left) and 40-50% (right) collision centrality as function of p_T . Statistical uncertainties are shown as bars and systematic uncertainties as boxes.

observed for v_3 and v_4 (not shown) but it is stressed that the observed scaling only holds approximately, as was also seen in [4].

4 Summary

Elliptic (v_2) and higher harmonic (v_3, v_4) flow coefficients of π^\pm , K^\pm , $p(\bar{p})$ and the ϕ -meson, measured in Pb—Pb collisions at $\sqrt{s_{NN}} = 5.02$ TeV, have been measured. Mass splitting is observed for $p_T < 2$ GeV/c, as well as approximate quark number scaling for $p_T > 2.5$ GeV/c. These high-precision measurements can be used to put new constraints on model calculations, furthering the understanding of the initial state of heavy-ion collisions, as well as of the transport coefficients and lifetime of the QGP.

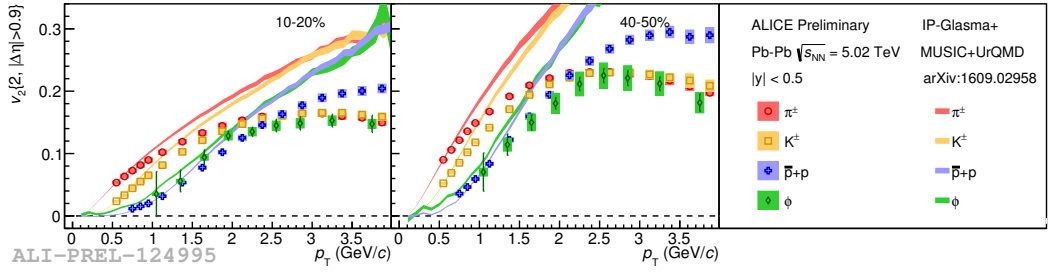


Figure 2. Flow coefficient v_2 of π^\pm , K^\pm , $p(\bar{p})$ and the ϕ -meson for 10-20% (left) and 40-50% (right) collision centrality compared to predictions from relativistic hydrodynamic calculations [9]. Statistical uncertainties are shown as bars and systematic uncertainties as boxes.

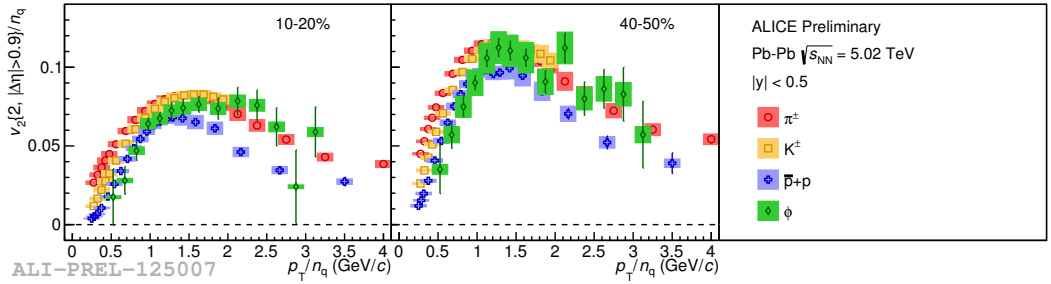


Figure 3. Scaling test for p_T -differential v_2 of π^\pm , K^\pm , $p(\bar{p})$ and the ϕ -meson for 10-20% (left) and 40-50% (right) collision centrality. The x - and y -axes are scaled by the number of constituent quarks n_q for each species independently. Statistical uncertainties are shown as bars, systematic uncertainties as boxes.

References

- [1] J. Adams et al. (STAR), Nucl. Phys. **A757**, 102 (2005)
- [2] J.Y. Ollitrault, Phys. Rev. **D46**, 229 (1992)
- [3] B. Abelev et al. (ALICE), Int. J. Mod. Phys. **A29**, 1430044 (2014)
- [4] B. Abelev et al. (ALICE), JHEP **06**, 190 (2015)
- [5] S.A. Voloshin, A.M. Poskanzer, R. Snellings (2008)
- [6] P. Huovinen, P.F. Kolb, U.W. Heinz, P.V. Ruuskanen, S.A. Voloshin, Phys. Lett. **B503**, 58 (2001)
- [7] D. Molnar, S.A. Voloshin, Phys.Rev.Lett. **91**, 092301 (2003)
- [8] G.Y. Qin, H. Petersen, S.A. Bass, B. Muller, Phys. Rev. **C82**, 064903 (2010)
- [9] S. McDonald, C. Shen, F. Fillion-Gourdeau, S. Jeon, C. Gale (2016)